

ORIGINAL ARTICLE

Pelizaeus Merzbacher disease: morphological analysis of the vestibulo-cochlear system

JOACHIM SCHMUTZHARD¹, ILONA SCHWENTNER¹, RUDOLF GLUECKERT¹, CONSOLATO SERGI², FELIX BECKMANN³, IRENE ABRAHAM¹, HERBERT RIECHELMANN¹, ANNELIES SCHROTT-FISCHER¹ & BERT MÜLLER⁴

¹Department of Otorhinolaryngology, and ²Institute of Pathology, Innsbruck Medical University, Austria, ³GKSS-Research Center, Institute for Materials Research, Geesthacht, Germany and ⁴Biomaterials Science Center, University of Basel, Switzerland

Abstract

Conclusion: In agreement with previously published findings, our results demonstrate that Pelizaeus Merzbacher disease (PMD) does not affect the development and morphology of the peripheral vestibulo-cochlear system. **Objective:** PMD is a consequence of X-linked mutation of the main central nervous system (CNS) myelin protein resulting in a complex neurological syndrome. Otorhinolaryngological symptoms include nystagmus and alterations of auditory-evoked brainstem responses. To date no histopathological analysis of the inner ear has been performed. **Materials and methods:** The temporal bone morphology of an affected fetus was examined with light microscopy and synchrotron radiation-based micro computed tomography. **Results:** The regular structure of the vestibulo-cochlear system was shown in this multi-modular analysis.

Keywords: *Histomorphology, synchrotron radiation-based micro computed tomography, cochlea, vestibulum*

Introduction

Friedrich Pelizaeus was the first to describe Pelizaeus Merzbacher disease (PMD) [1]. In 1910, Merzbacher published 14 further cases from the same family [2]. Today, PMD is known to arise from the X-linked mutation of the gene encoding for the myelin proto-lipid protein (PLP) [3–5]. PLP is the main central nervous system (CNS) myelin protein [6]. Its absence has been shown to be the basic pathophysiological mechanism of PMD [7]. Nystagmus and nystagmoid eye movements are among the validated observations. Furthermore, psychomotor deterioration, dystonia, progressive signs of upper motor neuron disease, and cerebellar dysfunction have been observed [8].

Feldman et al. [9–11] described otolaryngologic manifestations. In a case series of three infants who suffered from severe PMD, they observed inspiratory

stridor, necessitating intubation and later tracheotomy. Vocal cord paralysis was diagnosed in one patient. The second otorhinolaryngologic alteration was the pathologic auditory brainstem response (ABR) [11], showing only waves I and II. Further waves representing the brainstem and more afferent structures were not detectable [10]. This otologic finding could be explained by the basic characteristics of the disease. Nevertheless, no patho-morphologic study of PMD including expected changes in the inner ear morphology has been presented. Consequently, the temporal bone of a fetus (tested positive for the PLP 1 gene mutation) was examined by means of synchrotron radiation-based micro computed tomography (SR μ CT) and light microscopy. The present communication reveals the morphology of the temporal bone in 3D space with micrometer resolution.

Materials and methods

The study protocol was approved by the Internal Review Board of the Innsbruck Medical University (Ethics Committee resolution no. EK1: 06.10.06). The temporal bone was obtained during routine autopsy at the Institute of Pathology after legal interruption of pregnancy.

Background

The mother was a 27-year-old caucasian woman who was a known carrier of the PLP gene defect. Therefore a prenatal diagnosis of the PLP 1 mutation was performed. The chorionic villous sampling tested positive for the PLP 1 mutation and male gender. Following genetic counseling, an abortion was performed in the 16th week of gestation. The pathologic work-up of the fetus confirmed the diagnosis of a manifested PMD.

Multi-modular work-up

Light microscopy and SR μ CT were used to uncover the morphology of the temporal bone. This examination focused on the histologic examination of the cochlea with special emphasis on the neural structures and on the 3D visualization of the temporal bone with SR μ CT.

Specimen preparation for light microscopy

Specimens were fixed in Karnovsky's fixative (5% glutaraldehyde and 4% paraformaldehyde in cacodylate buffer) for several weeks. Subsequently, they were washed in 0.1 M cacodylate buffer and post-fixed with 1% osmium tetroxide in 0.05 M cacodylate buffer for 1 h at 4°C. The excess osmium tetroxide was removed by rinsing the specimens four times (15 min each) in 0.1 M cacodylate buffer. The orientation of the cochlea was done with the help of the oval and round window and the inner acoustic meatus. Decalcification with 10% EDTA (Titriplex III[®], Merk, Darmstadt, Germany) was carried out for 4 weeks.

After passing through a graded series of ethanol, methyl benzoate, and chloroform, paraffin embedding was performed and 5 μ m radially aligned paraffin serial sections were produced and stained with hematoxylin and eosin (H&E).

Digital images of the sections were acquired using an Olympus BX 50 light microscope with a CCD video camera (Sony DXC-950P) linked to the Imagepro[®] 6.0 analysis system (Media Cybernetics[®], Silver Spring, USA).

Synchrotron radiation-based micro computed tomography

The specimen was treated with 1% osmium tetroxide in 0.05 M cacodylate buffer at 4°C for 1 h.

The SR μ CT data were acquired at the beamline BW 2 (HASYLAB at DESY, Hamburg, Germany) in an absorption contrast set-up [12] operated by the GKSS-Research Center, Geesthacht, Germany. At the photon energy of 18.0 keV 1441 projections between -180° and 180° were recorded at an optical magnification of 2.27 taking advantage of the asymmetric rotation axis. Therefore, the pixel size of the projections corresponded to $4 \times 4 \mu\text{m}^2$. The spatial resolution of the entire tomography set-up was experimentally characterized by the modulation transfer function [13] and was found to be 6.98 μm . To reach this spatial resolution of the entire specimen it was necessary to combine four datasets based on the registration with voxel precision. Since the monochromatic X-ray beam is almost perfectly parallel, the tomograms have been reconstructed slice-wise by means of the filtered back-projection algorithm [14].

Image processing of the SR μ CT data

The software VG Studio Max 1.2.1 (Volume Graphics, Heidelberg, Germany) was used for segmenting and visualizing the anatomy of the embedded cochlea. To calculate the length of the cochlea a tool was developed in IDL 7.0 (ITT Visual Information Solutions, Boulder, CO, USA) that allows for manual selection of a series of points within the 3D dataset. This trajectory can be highlighted with defined diameter in the 3D volume and is finally visualized by means of the VG Studio software. The length of the trajectory defines here the length of the cochlea.

Results

Before the specimen was cut for histological analysis, non-destructive SR μ CT was carried out. The 3D data uncovered a cochlea with two and a half turns, as illustrated in Figure 1. For deeper analysis a trajectory was semi-automatically selected as the center line of the cochlear duct. The length of this line along the two and a half turns corresponded to 25.58 mm. Analyzing the spiral ganglion the Rosenthal's canal with neuronal structures come to light, as shown in Figure 2. The trajectory placed in the center of the Rosenthal's canal showed the expected 1.5 turns with a length of 8.54 mm (Figure 1). The 3D presentation of the vestibular organ (Figure 3) demonstrated that the three semicircular canals denoted a healthy configuration.



Figure 1. Based on the 3D SR μ CT dataset the center lines (trajectories) of the cochlear duct (red) and of the Rosenthal canal (yellow) are represented together with the virtual cut lateral through the cochlea.

The subsequently performed histologic examination also revealed a fully developed cochlea: The cochlear duct consisted of two and a half turns. The well-developed scala tympani and scala vestibuli were identified. The modiolus matched the expected size and shape. The spiral ganglion showed the characteristic configuration (Figure 4A and D). The

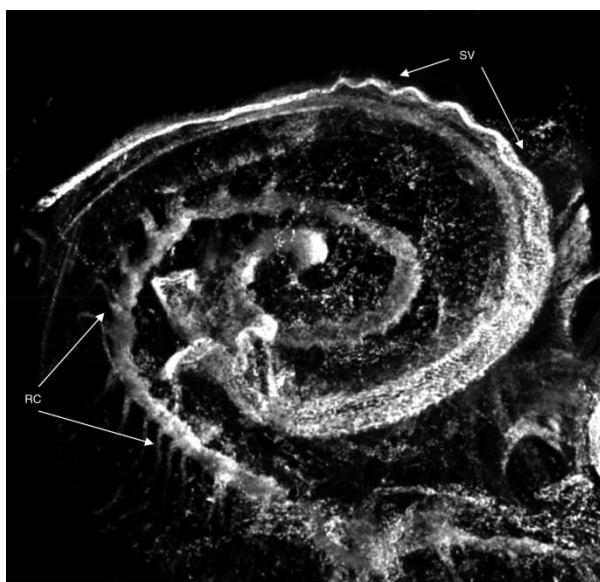


Figure 2. Based on the SR μ CT data a part of the stria vascularis (SV) and the full expansion of the Rosenthal canal (RC) with the neuronal structures of the spiral ganglion are visualized.



Figure 3. This 3D view of the vestibular organ shows the cross-sections of the superior semicircular canal (SSC) and of the posterior semicircular canal (PSC) as well as a full view of the lateral semicircular canal (LSC).

microscopic images of the cochlear nerve illustrated its regular morphology. The vestibular system showed a well-developed sensoneural epithelium (Figure 4C). Three semicircular canals that were well developed in size and configuration could be extracted. Both the vestibular nerve and the scarpa ganglion were fully emerged (Figure 4A and B). Because the specimen fixation was compromised, the cellular structures of the organ of Corti, stria vascularis, and the semicircular canals were not described in detail. The fixation of the neuronal structures, however, was successful and allowed adequate analysis.

Discussion

The ABR [11] and the findings in vestibular studies [9] clearly demonstrate the functional otorhinolaryngological alterations found in PMD patients. However, these clinical results did not include morphology of the temporal bone and the vestibulo-cochlear system. In the temporal bone investigated, SR μ CT revealed normally configured gross anatomic vestibulo-cochlear structures. The histologic analysis showed regularly configured neuronal structures of the cochlear and vestibular system. The sensoneural epithelium was regularly developed. The cochlear structures could not be fully evaluated. The use of 1% OsO₄ post-fixation to enhance the contrast (density resolution) in SR μ CT permitted

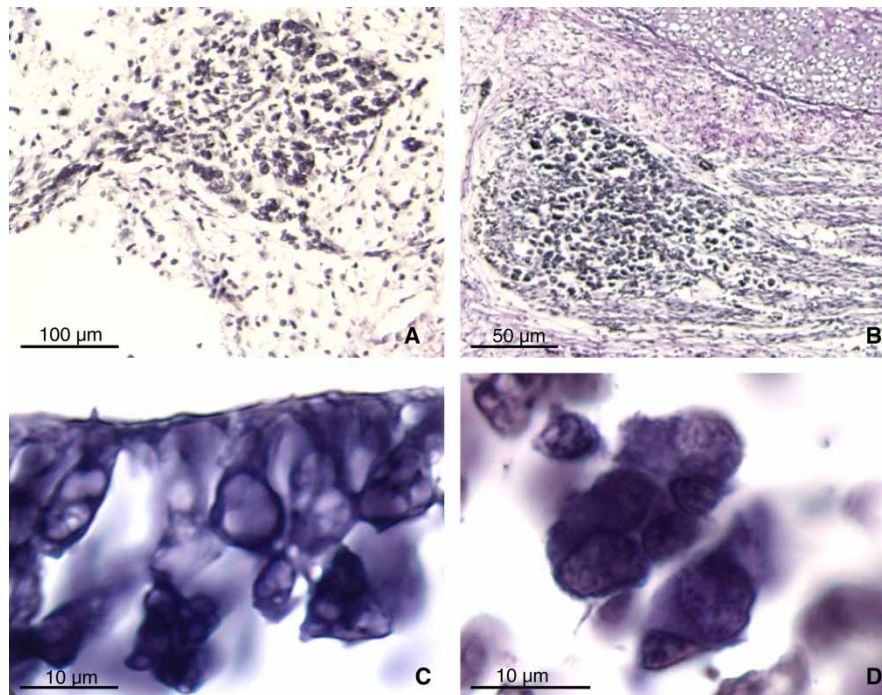


Figure 4. (A) An overview of the spiral ganglion (osmium tetroxide fixation and H&E staining; original magnification $\times 40$). (B) An overview of the vestibular ganglion (osmium tetroxide fixation and H&E staining; original magnification $\times 100$). (C) The sensoneural epithelium of the vestibular end organ (osmium tetroxide fixation and H&E staining; original magnification $\times 1000$). (D) A ganglion cell of the spiral ganglion (osmium tetroxide fixation and H&E staining; original magnification $\times 1000$).

detailed visualization of the Rosenthal's canal with its neuronal content. This post-fixation, however, prevented immunohistochemical staining for the myelin PLP [15], which represents the basic pathological defect.

Kaga et al. [10] published results on the pure tone audiometry thresholds in PMD patients. In their case series they described a hearing threshold ranging from normal to mild hearing loss of 35 dB. Therefore, alterations of the ABR seemed to be more important. The fundamental pathologic defect of the central myelin sheath can explain the ABR – characteristics with regular behavior in wave I and II, representing the peripheral part of the auditory system and missing waves III–V, representing the central part of the auditory system [10,11]. These clinical results fit very well with the morphological findings of the present communication, revealing an unaffected spiral ganglion and a regularly configured gross anatomical cochlea. The other symptoms usually associated with the PMD are nystagmus and ataxia [15]. The vestibular studies revealed several central electronystagmographic abnormalities, such as the failure of fixation suppression, poor smooth pursuit, and impaired performance of optokinetic nystagmus at high stripe speeds [9]. These results verify the central nervous origin of the nystagmus and match with the present findings, which do not show any pathologic alteration.

Conclusion

The SR μ CT data and the histologic images demonstrate that the gross morphology of the vestibulo-cochlear system in PMD is regularly developed with unaffected vestibular structures. In line with the previously published clinical data [9–11] one can obviously conclude that PMD does not affect the development and function of the peripheral vestibular system and the gross anatomical development of the cochlear system.

Acknowledgement

The authors acknowledge the support of J. Herzen (Hamburg) during the data acquisition. HASYLAB at DESY kindly provided beamtime at BW 2 (II-20060035 EC). The work was supported by the Austrian Science Foundation (FWF Project B05 15958).

Declaration of interest: The authors report no conflicts of interest. The authors alone are responsible for the content and writing of the paper.

References

- [1] Pelizaeus R. Über eine eigentümliche Form spastischer Lähmungen mit Zerebralerscheinungen auf hereditärer Grundlage. Arch Psychiat Nervenkr 1885;16:698–710.

- [2] Merzbacher L. Eine eigenartige familiär-hereditäre Erkrankungsform (Aplasia axialis extracorticalis congenita). *Zeitsch Ges Neurol Psychiat* 1910;3:1–138.
- [3] Gencic S, Abuelo D, Ambler M, Hudson LD. Pelizaeus-Merzbacher disease: an X-linked neurologic disorder of myelin metabolism with a novel mutation in the gene encoding proteolipid protein. *Am J Hum Genet* 1989;45:435–42.
- [4] Hudson LD, Puckett C, Berndt J, Chan J, Gencic S. Mutation of the proteolipid protein gene PLP in a human X chromosome-linked myelin disorder. *Proc Natl Acad Sci U S A* 1989;86:8128–31.
- [5] Trofatter JA, Dlouhy SR, DeMyer W, Conneally PM, Hodes ME. Pelizaeus-Merzbacher disease: tight linkage to proteolipid protein gene exon variant. *Proc Natl Acad Sci U S A* 1989;86:9427–30.
- [6] Folch J, Lees M. Proteolipides, a new type of tissue lipoproteins; their isolation from brain. *J Biol Chem* 1951;191:807–17.
- [7] Zeman M, DeMyer W, Falls HF. Pelizaeus-Merzbacher Disease. A study in nosology. *J Neuropathol Exp Neurol* 1964;23:334–54.
- [8] Koeppen AH, Ronca NA, Greenfield EA, Hans MB. Defective biosynthesis of proteolipid protein in Pelizaeus-Merzbacher disease. *Ann Neurol* 1987;21:159–70.
- [9] Mallinson AI, Longridge NS, Dunn HG, McCormick AQ. Vestibular studies in Pelizaeus-Merzbacher disease. *J Otolaryngol* 1983;12:361–4.
- [10] Kaga K, Tamai F, Kodama M, Kodama K. Three young adult patients with Pelizaeus-Merzbacher disease who showed only waves I and II in auditory brainstem responses but had good auditory perception. *Acta Otolaryngol* 2005;125:1018–23.
- [11] Feldman JL, Kearns DB, Seid AB, Pransky SM, Jones MC. The otolaryngologic manifestations of Pelizaeus-Merzbacher disease. *Arch Otolaryngol Head Neck Surg* 1990;116:613–6.
- [12] Beckmann F. Microtomography using synchrotron radiation as a user experiment at beamlines BW2 and BW5 of HASYLAB at DESY. *Proc SPIE* 2002;4503:34–41.
- [13] Müller B, Thurner P, Weitkamp T, Rau C, Bernhardt R, Karamuk E, et al. Non-destructive three-dimensional evaluation of biocompatible materials by microtomography using synchrotron radiation. *Proc SPIE* 2001;4503:178–88.
- [14] Kak AC, Slaney M. Principles of computerised tomographic imaging. New York: IEEE Press; 1988.
- [15] Garbern JY. Pelizaeus-Merzbacher disease: genetic and cellular pathogenesis. *Cell Mol Life Sci* 2007;64:50–65.